JOURNAL OF TISSUE ENGINEERING AND REGENERATIVE MEDICINE
J Tissue Eng Regen Med 2010; **4**: 349–355.
Published online 7 January 2010 in Wiley InterScience (www.interscience.wiley.com) **DOI:** 10.1002/term.245

RESEARCH ARTICLE

Silk fibroin microparticles as carriers for delivery of human recombinant BMPs. Physical characterization and drug release

P.C. Bessa[1,2,3,4]*, E.R. Balmayor[1,2], H.S. Azevedo[1,2], S. Nürnberger[4], M. Casal[3], M. van Griensven[4], R.L. Reis[1,2] and H. Redl[4]

[1]*3B's Research Group - Biomaterials, Biodegradables and Biomimetics, University of Minho, Headquarters of the European Institute of Excellence on Tissue Engineering and Regenerative Medicine, AvePark, 4806-909 Taipas, Guimarães, Portugal*
[2]*IBB – Institute for Biotechnology and Bioengineering, PT Associated Laboratory, Guimarães, Portugal*
[3]*CBMA – Centro de Biologia Molecular e Ambiental, Department of Biology, University of Minho, Campus de Gualtar, 4710-057 Braga, Portugal*
[4]*Ludwig Boltzmann Institute for Experimental and Clinical Traumatology, in the AUVA research center, Austrian Cluster for Tissue Regeneration, Donaueschingenstrasse 13, 1200, Vienna, Austria*

Abstract

Bone morphogenetic proteins (BMPs) are cytokines with strong ability to promote new bone formation. Herein, we report the use of silk fibroin microparticles as carriers for the delivery of BMP-2, BMP-9 or BMP-14. BMP-containing fibroin microparticles were prepared by a mild methodology using dropwise addition of ethanol, exhibiting mean diameters of 2.7 ± 0.3 μm. Encapsulation efficiencies varied between 67.9 ± 6.1 % and 97.7 ± 2.0 % depending on the type and the amount of BMP loaded. Release kinetics showed that BMP-2, BMP-9 and BMP-14 were released in two phases profile, with a burst release in the first two days followed by a slower release, for a period of 14 days. The release data were best explained by Korsmeyer's model and the Fickian model of drug diffusion. Silk fibroin microparticles can offer a promising approach for the sustained delivery of different BMPs in tissue engineering applications. Copyright © 2010 John Wiley & Sons, Ltd.

Received 20 June 2009; Accepted 11 November 2009

Keywords bone morphogenetic protein; silk fibroin; microparticles; drug delivery; BMP-2; BMP-9; BMP-14

1. Introduction

Bone morphogenetic proteins (BMPs) have recently sparked great interest in the tissue engineering field due to their strong ability to promote new bone and cartilage formation (Reddi, 2005; Bessa *et al*., 2008a). Different materials have been proposed as carriers for BMPs (Bessa *et al*., 2008b). Carriers are used to increase the lifetime, stability and bioactivity of the BMPs and release these growth factors in both timely and site-specific sustained ways. Microparticles as carriers can offer the advantages of a controlled release, protecting the protein from loss of bioactivity and targeting the delivery into the specific injury site, with no dispersion into surrounding tissues.

Several different microparticulated systems have been investigated for the delivery of BMPs, most based on polylactic-co-glycolic acid (PLGA) (Lee *et al*., 1994; Phillips *et al*., 2006; Wei *et al*., 2007), on collagen (Wang *et al*., 2003, Itoh *et al*., 2004) or on dextran (Chen *et al*., 2006, 2007). Silk is an attractive choice as a material for bone tissue engineering, due to being biocompatible, slowly biodegradable and possessing excellent mechanical properties such as tensile strength and rigidity which are

*Correspondence to: P.C. Bessa, Ludwig Boltzmann Institute for Experimental and Clinical Traumatology, Donaueschingenstrasse 13, 1200, Vienna, Austria.
E-mail: paulo.bessa@dep.uminho.pt

highly desirable for a potential use as a scaffold for bone tissue engineering (Scheibel 2006). Silk fibroin has been investigated as a carrier for BMPs in several contributions by Kaplan and colleagues, in form of membranes for healing cranial defects in mice (Karageorgiou *et al*., 2004), electrospun nanofibers (Li *et al*., 2006), and scaffolds used for critical size defects in rats (Kirker-Head *et al*., 2007) and mice (Karageorgiou *et al*., 2006).

Fibroin has been recently described to produce microparticles when precipitated with ethanol at specific fibroin concentrations and freeze temperature (Nam and Park, 2001; Cao *et al*., 2007; Zhang *et al*., 2007). Ethanol causes a shift in the random coil structure of fibroin to an insoluble beta-sheet configuration (Nam and Park, 2001). The addition of ethanol to the fibroin solution causes it to either precipitate to form a gel that can be used as a scaffold for tissue engineering (Nazarov *et al*., 2004; Tamada, 2005) or to form a gel consisting of micrometric particles (Nam and Park, 2001; Zhang *et al*., 2007). If these variables are controlled, a control of particle size is possible and could be adapted to specific clinical applications. Therefore, we were interested in using this system as a possible delivery micro-carrier for BMPs.

This study explores the use of silk fibroin microparticles as a potential delivery system for the release of different BMPs. Fibroin microparticles were produced under very mild conditions, with a concomitant loading of BMP-2, BMP-9 or BMP-14. Besides the fact that BMP-2 has been widely researched as a osteogenic factor (Bessa *et al*., 2008b), we also evaluated the potential of the fibroin particles to deliver BMP-9 and BMP-14 due to their potential in novel therapeutical applications. BMP-9 is reported to be one of the most osteogenic BMPs (Kang *et al*., 2004) and BMP-14 is used in tendon and ligament regeneration (Nakamura *et al*., 2003; Dines *et al*., 2007), in spinal fusion (Spiro *et al*., 2001), bone formation (Simank *et al*., 2004; Kadamatsu *et al*., 2008) and is critical for digit and limb development (Merino *et al*., 1999). The particles were characterized for morphology, size distribution, water uptake, encapsulation efficiency and the release kinetics of the three BMPs, with different amounts of loaded growth factor.

2. Materials and methods

2.1. Materials

Silk containing *Bombyx mori* cocoons were purchased from Halcyon Yarn, US. Human BMP-2, expressed in Chinese Hamster Ovary (CHO) cells, was purchased from Wyeth, UK. Human BMP-9 and BMP-14 were cloned and expressed in *Escherichia coli*, purified by histidine-tag affinity chromatography and freeze-dried, as described elsewhere (Bessa *et al*., 2009). All chemicals were of analytical grade and used as received.

2.2. Methods

2.2.1. Preparation of BMP silk fibroin microparticles

Isolation of silk fibroin from Bombyx mori cocoons. Silk fibroin was isolated from *Bombyx mori* cocoons following a degumming protocol with modifications (Zhang *et al*., 2007). Briefly, the cocoon shells of silkworm *Bombyx mori* were degummed twice in a boiling solution of 0.5% Na_2CO_3 for 0.5 h, at 90 °C, and the resulting degummed fibers were subsequently dissolved, in a ternary system, i.e. a mixed solution of calcium chloride, ethanol and water ($CaCl_2/C_2H_5OH/H_2O$: 1 : 2 : 8 mole ratio) at 90 °C for 6 h. The solution was then filtered (0.22 m, Rotilab, Germany), and the solution was extensively dialyzed, using a cellulose semi-permeable (molecular weight cut-off = 12 000 kDa) membrane, against distilled water to remove $CaCl_2$, smaller molecules and impurities. The fibroin was lyophilized and used for the preparation of microparticles.

Microparticle preparation. Silk fibroin microparticles were prepared by ethanol precipitation according to the method described by Cao *et al*. (2007), with modifications. A solution of 1% (w/v) silk fibroin in phosphate buffer saline (PBS, pH 7.4) was prepared (5 ml) and filtered with a 0.22 m PVDF membrane (Rotilab, Germany). For preparation of BMP loaded particles, 5 or 50 g/ml of growth factor (either BMP-2, BMP-9 or BMP-14) were added to the fibroin suspension, corresponding to a smaller or a larger dose of loaded BMP (0.5 or 5 g of BMP per mg of fibroin, respectively). The solution was incubated at room temperature with stirring (600 rpm) for 20 min. Absolute ethanol was added dropwise to a ratio of 1 : 2 to the initial volume of silk fibroin, and the solution incubated overnight at −20 °C. Different ratios (ethanol to initial volume of fibroin suspension) were also tested to investigate the change in particle size. The resulting microparticles were collected by centrifugation at 4000 g, 4 °C, for 5 min, washed twice with distilled water and lyophilized, after snap-freezing in liquid nitrogen, in a Christ Alpha 1–4 (Linder, Austria) lyophilizer. Sterile conditions were used during the entire procedure.

2.2.2. Physical characterization

Scanning electron microscopy (SEM). Fibroin particles were morphologically characterized by scanning electron microscopy (SEM). SEM analysis was performed on gold-coated air-dried samples (Agar Sputercoater 108, Essex, UK) and using a Philips XL20 microscope (Philips, Eidhoven, The Netherlands). Particle size measurements were obtained from different micrographs acquired in the SEM.

Size distribution. Measurements of particle size were performed on freshly prepared samples by dynamic light

DOI: 10.1002/term

scattering (DLS), using a Zetasizer NanoZS (Malvern, UK). For the analysis, each sample was diluted to an appropriate concentration with ultrapure (filtered) water. Each analysis lasted 60 s and was performed at 25 °C.

Water uptake and degradation studies. The hydration degree of unloaded fibroin microparticles was evaluated after immersion into PBS, at 37 °C, for periods up to 30 days (30 min, 4 h, 24 h, 2 d, 5 d, 8 d, 14 d, 21 d and 30 d). The weight loss of unloaded fibroin particles was assessed after immersion into PBS, at 37 °C, for periods up to 30 days (1 d, 2 d, 5 d, 8 d, 14 d and 30 d). All experiments were performed in triplicate. Percentage of water uptake (WU) after each time period of immersion (t) was calculated using the following equation:

$$\mathrm{WU}\ (\%) = \frac{(\mathrm{W}_w - \mathrm{W}_j)}{\mathrm{W}_i} \times 100$$

The percentage of mass remaining (MR) after each time period (t) was calculated using the following equation:

$$\mathrm{WL}(\%) = \frac{\mathrm{W}_d}{\mathrm{W}_i} \times 100$$

'W_w' and 'W_d' correspond, respectively, to the weight of fibroin particles in wet state (after removal from solution, washing with distilled water and soft-blotting with filter paper) and dry state (after removal of solution, washing after distilled water and freeze-drying); 'Wi' correspond to the initial dry weight of particles, before immersion.

2.2.3. In vitro drug release studies

Quantification of protein. For measurement of BMP-2 concentration, a BMP-2 sandwich-type ELISA kit (Eubio, Austria) was used, following the manufacturer's instructions. A calibration curve was obtained using standard preparations of BMP-2 of known concentration. For detection of BMP-9 and BMP-14, the sample concentrations were estimated by dot blot with the use of an anti-histidine tag antibody (Sigma, US). The blot intensities were compared with standards of known concentration, using image analysis (ChemiImage 4400, Alpha Innotech, US).

Determination of loading capacity and encapsulation efficiency. The microparticle encapsulation efficiency was determined upon their separation from the aqueous preparation medium containing the non-associated protein (free BMP) by centrifugation (10 000 g, 10 min). Theoretical drug content (total BMP) was calculated assuming that the entire amount of drug added to the fibroin solution was encapsulated and no drug loss occurred at any stage of the particle preparation. All experiments were performed in triplicate. The microparticle encapsulation efficiency (E.E.) and BMP loading capacity (L.C) were calculated using the following equations:

$$\mathrm{E.E.}(\%) = \frac{\text{Total BMP amount}(\ \mathrm{g}) - \text{Free BMP amount}(\ \mathrm{g})}{\text{Total BMP amount}} \times 100$$

$$\mathrm{L.C.}(\ \mathrm{g\ BMP/mg\ particles}) = \frac{\text{Total BMP amount}(\ \mathrm{g}) - \text{Free BMP amount}(\ \mathrm{g})}{\text{Microparticles weight(mg)}}$$

In vitro release. Silk fibroin particles loaded with BMP-2, BMP-9 or BMP-14 (initial loading of 0.5 or 5 g/mg) were suspensed in 5 ml PBS (pH 7.4), at 37 °C, with 200 rpm agitation, to a concentration of 2 mg/ml of microparticles. At pre-determined time points (1 h, 4 h, 1 d, 2 d, 4 d, 8 d and 14 d), 250 l of solution was removed, centrifuged (10 000 g, 10 min) and filtered in 0.22 m membranes and stored at −20 °C until quantification. The volume of solution removed was replaced with fresh buffer. Sterile conditions were applied to prevent any contamination of samples. All experiments were performed in triplicate. Percentage of release was obtained by comparing the measured growth factor content with the actual loading capacity.

Release kinetics models. To study the release kinetics, the data obtained from the *in vitro* release was treated accordingly to zero order as cumulative amount of drug released *vs*. time (equation 1), first order as log cumulative percent drug remaining *vs*. time (equation 2), Higuchi kinetics as cumulative percent drug released *vs*. square root of time (equation 3) and Korsmeyer kinetics as log cumulative percent drug released *vs*. log time (equation 4) (Huguchi, 1963; Chowdary and Ramesh, 1993; Hadjiioannou *et al*., 1993; Bourne, 2002):

$$\mathrm{R} = \mathrm{k}_1 \mathrm{t} \quad (1)$$

$$\mathrm{Log\ UR} = \mathrm{k}_2 \mathrm{t}\ 2.303 \quad (2)$$

$$\mathrm{R} = \mathrm{k}_3 \mathrm{t}\ 0.5 \quad (3)$$

$$\mathrm{Log\ R} = \log \mathrm{k}_4 + \mathrm{n} \log \mathrm{t} \quad (4)$$

where R and UR are released and unreleased percentages, respectively, at time (t); k_1, k_2, k_3 and k_4 are the rate constants of zero-order, first order, Higuchi and Korsmeyer models, respectively; n is a exponent that characterizes the mechanism of release.

DOI: 10.1002/term

2.2.4. Statistical analysis

Experiments were performed in triplicate ($n = 3$) and mean ± standard deviations were reported. Student's t test was used for statistical analysis using a two-tailed paired test. Statistical significance was defined as $p < 0.01$ for a 99% confidence.

3. Results

3.1. Morphology, size distribution and encapsulation efficiency

The morphology of fibroin particles observed by SEM is shown in Figure 1. Fibroin formed spherical microparticles with diameters increasing when the ratio of ethanol to silk solution (used during the preparation of particles) increased. The particles had mean sizes of 580.0 ± 120.6 nm using a 1 : 2 ratio of ethanol and silk, increasing up to 1.1 ± 0.3 m with a 1 : 3 ratio ($p < 0.01$), and to 1.2 ± 0.4 m with 1 : 4 ratio (not significant). Using size distribution, the particles, using a 1 : 2 ratio, showed an average size of 2.7 ± 0.3 m, in wet state (Figure 2). The largest part of microspheres (88.5%) had sizes ranging from 1.5 to 3.0 m in diameter. The encapsulation efficiency of BMP-2 into the fibroin particles was 97.7 ± 2.0 % per total amount of growth factor added during the preparation of the particles, when 0.5 g BMP-2 (per mg fibroin) was loaded, and 76.8 ± 3.5 %, when 5.0 g of BMP-2 were loaded (Table 1). The loading capacity was 0.69 ± 0.06 g of BMP-2 per mg of fibroin particles, and 5.4 ± 0.5 g of BMP-2 per mg of particles, when the different amounts were loaded. For BMP-9, the encapsulation efficiency was 90.2 ± 5.9 % and 72.4 ± 4.4 %, and the loading capacity was 0.63 ± 0.17 and 5.1 ± 0.5 g/mg of particles, when 0.5 or 5.0 g BMP-9 were loaded, respectively. For BMP-14, the encapsulation efficiency was 82.5 ± 6.0 % and 67.9 ± 6.1 %, and the loading capacity was 0.60 ± 0.17 and 4.8 ± 0.6 g of BMP-14 per mg of particle weight, when 0.5 or 5.0 g BMP-14 were loaded, respectively.

3.2. Water uptake and degradation studies

The swelling occurred rapidly during the first two days of immersion, up to 48.5 ± 6.7 % after 30 min and up to 167.7 ± 14.1 % after day 2 ($p < 0.01$), with water uptake reaching a peak at day 8 with 227.7 ± 26.6 % ($p < 0.01$) (Figure 3). This was followed by a slow and gradual decline in wet weight, with a swelling value of 203.4 ± 25.0 % (non-significant) after day 30, possibly due to weight loss. The remaining mass was 97.1 ± 1.5 % after day 5, 95.4 ± 2.5 % after day 14, and 93.5 ± 3.3 % after day 30 (Figure 4).

3.3. *In vitro* release studies

Drug release studies were evaluated when fibroin particles loaded with BMP-2, BMP-9 and BMP-14 were immersed in PBS, at 37 °C, with agitation. The microparticles loaded with 0.5 g of BMPs/mg fibroin, showed an initial burst release with more than half of protein being released during the first two days (64.1 ± 5.1 % for BMP-2, 78.4 ± 7.9 % for BMP-9 and 62.5 ± 7.3 % for BMP-14),

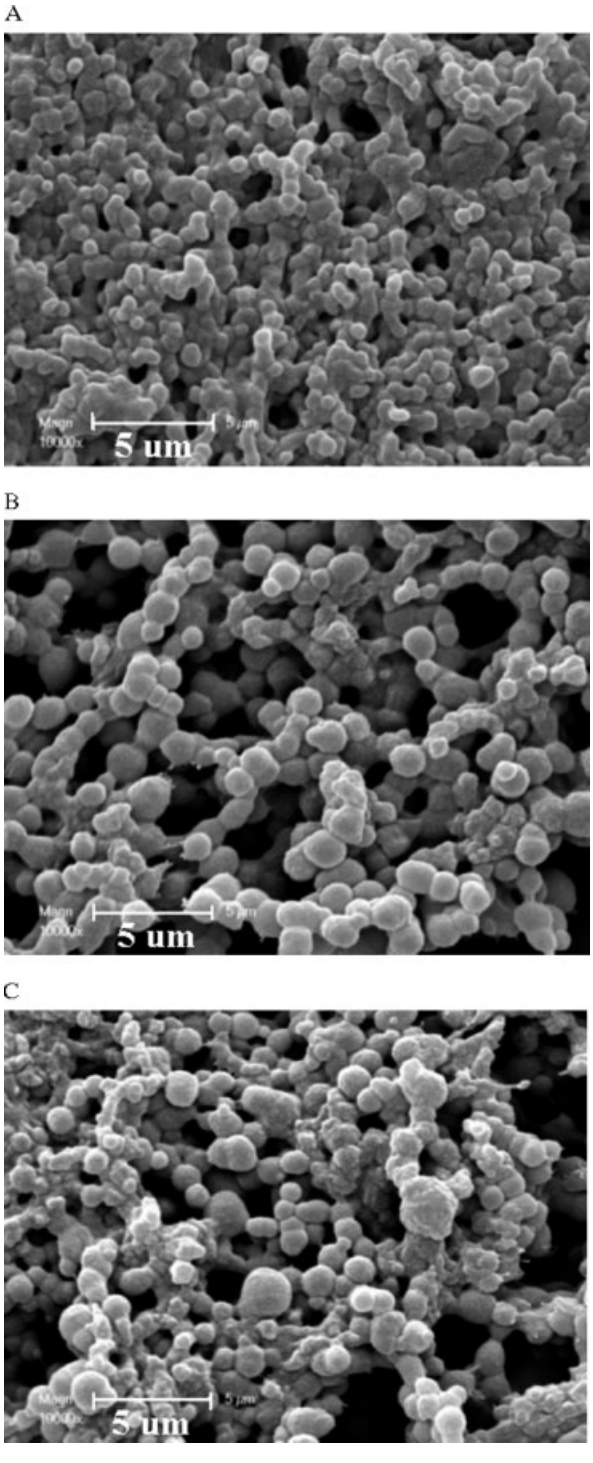

Figure 1. SEM micrographs of unloaded fibroin microparticles, produced with different ethanol : silk solution ratios: A) 1 : 2 ratio, B) 1 : 3 ratio, and C) 1 : 4 ratio. Magnification 10.000 x. Scale 5 μm

DOI: 10.1002/term

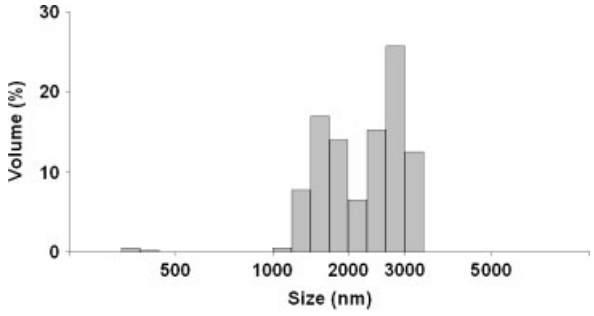

Figure 2. Size distribution of unloaded silk fibroin particles. Almost all particles showed sizes ranging between 2 and 3 μm, with a mean diameter of 2.7 ± 0.3 μm. Size refers to particle diameter (nanometers)

Table 1. Loading and encapsulation efficiencies of BMP-loaded fibroin microparticles (mean ± SD, $n = 3$)

Growth factor	Amount of growth factor/mg fibroin, prior to loading (g)	Encapsulation efficiency (%)	Loading capacity (g BMP/mg particles)
BMP-2	0.5	97.7 ± 2.0	0.69 ± 0.06
BMP-9	0.5	90.2 ± 5.9	0.63 ± 0.17
BMP-14	0.5	85.8 ± 6.0	0.60 ± 0.17
BMP-2	5.0	76.8 ± 3.5	5.4 ± 0.5
BMP-9	5.0	72.4 ± 4.4	5.1 ± 0.5
BMP-14	5.0	67.9 ± 6.1	4.8 ± 0.6

Encapsulation efficiency (%) = {[total BMP amount (g) −free BMP (g)]/total BMP (g)} × 100. Loading capacity (g BMP/mg particles) = {[total BMP amount (g) −free BMP (g)]/microparticles weight (mg)}.

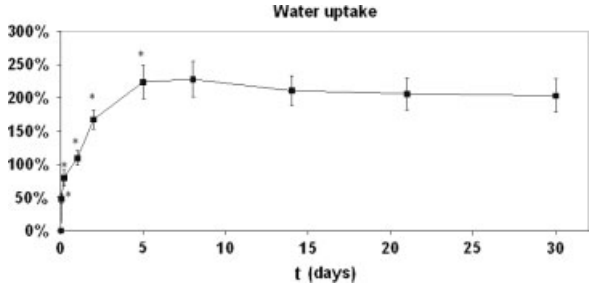

Figure 3. Evolution of water uptake behavior of unloaded silk fibroin microparticles in phosphate buffer saline as a function of immersion time (t). (mean ± SD, $n = 3$). Water uptake increased significantly up to 5 days, peaked after 8 days, and then slightly declined (non-significantly). * $p < 0.01$ related to the difference between consecutive time measurements

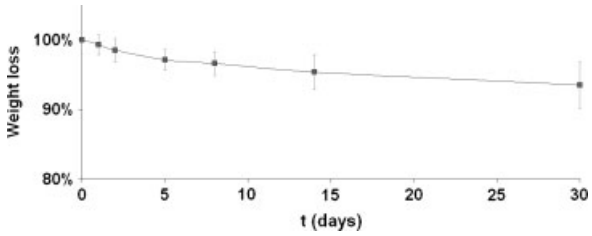

Figure 4. Evolution of weight loss of unloaded fibroin particles in phosphate buffer saline as a function of immersion time (t). (mean ± SD, n = 3). The remaining mass decreased to 97.1 ± 1.5 % after day 5, 95.4 ± 2.5 % after day 14, and 93.5 ± 3.3 % after day 30

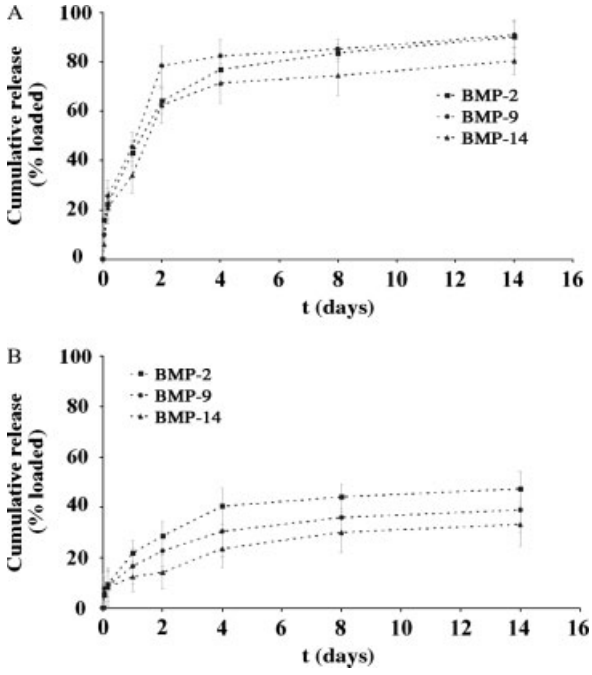

Figure 5. Release kinetics of BMP-2, BMP-9 and BMP-14 immobilized in fibroin particles. ELISA was used for BMP-2 quantification and dot-blot for BMP-9 and BMP-14 quantification (Mean ± SD, $n = 3$). A) Release from particles containing 0.5 μg of BMP per mg of fibroin; B) release from particles containing 5.0 μg of BMP per mg of fibroin. Cumulative release is expressed in percentage of loaded protein

followed by a second phase of a slower and more sustained release with 90.1 ± 6.9 % of BMP-2, 90.9 ± 5.2 % of BMP-9, and 80.4 ± 5.6% of BMP-14, released after 14 days (Figure 5A). This corresponds to a release rate, of 15 ng/day, 7 ng/day and 8 ng/day (per mg of fibroin), between day 2 and 14, for each BMP, after a burst release of 442 ng, 499 ng and 377 ng of each BMP (in 2 days).

The particles loaded with 5 g/mg of BMPs showed an initial release of about 28.6 ± 5.5 % of BMP-2, 22.7 ± 6.3 % of BMP-9 and 14.1 ± 6.7 % of BMP-14 being released after two days (Figure 5B), which corresponds to 1.5 g, 1.1 g and 0.7 g of each growth factor. After 14 days, 47.3 ± 7.0 % BMP-2, 38.9 ± 8.9 % BMP-9, and 33.2 ± 8.8 % BMP-14 were released, corresponding to a release rate of 86 ng/day, 72 ng/day and 76 ng/day, for each BMP. At the end of this period, 2.5 g, 2.0 g and 1.5 g of each growth factor were (cumulatively) released from the particles (per mg of fibroin).

The release data of the BMPs were treated accordingly to first order, Higuchi and Korsmeyer equations (Table 2) and zero order equation (data not shown). The release data of BMP-2, BMP-9 and BMP-14 were best explained by Korsmeyer's equation (r^2 varying between 0.92 and 0.98), followed by Higuchi's equation (r^2 varying between 0.75 and 0.95) and by first order kinetics (r^2 varying between 0.71 and 0.91). The release exponent "n" of Korsmeyer's model, varied in the different experimental conditions between 0.30 and 0.42. Since n<0.43 the release data

DOI: 10.1002/term

Table 2. Release kinetics of BMPs immobilized in fibroin particles

Growth factor	Amount of growth factor/ mg fibroin, prior to loading (g)	Equation modelling
BMP-2	0.5	$y = -0.057x + 1.7547; r^2 = 0.91$[a]
		$y = 17.926x + 26.183; r^2 = 0.85$[b]
		$y = 0.3029x + 1.6459; r^2 = 0.97, n = 0.30$[c]
BMP-9	0.5	$y = -14.148x + 25.648; r^2 = 0.71$[a]
		$y = 19.509x + 25.325; r^2 = 0.75$[b]
		$y = 0.3674x + 1.6277; r^2 = 0.92, n = 0.37$[c]
BMP-14	0.5	$y = -0.0344x + 1.8002; r^2 = 0.70$[a]
		$y = 18.232x + 17.785; r^2 = 0.80$[b]
		$y = 0.4195x + 1.519; r^2 = 0.92, n = 0.42$[c]
BMP-2	5.0	$y = -0.0133x + 1.9131; r^2 = 0.71$[a]
		$y = 11.018x + 8.4402; r^2 = 0.88$[b]
		$y = 0.385x + 1.2845; r^2 = 0.98, n = 0.39$[c]
BMP-9	5.0	$y = -77.226x + 150.34; r^2 = 0.77$[a]
		$y = 8.5682x + 7.496; r^2 = 0.92$[b]
		$y = 0.301x + 1.2361; r^2 = 0.96, n = 0.30$[c]
BMP-14	5.0	$y = -0.0083x + 1.9499; r^2 = 0.83$[a]
		$y = 7.2919x + 5.3548; r^2 = 0.95$[b]
		$y = 0.2978x + 1.1429; r^2 = 0.97, n = 0.30$[c]

[a]First order (log cumulative percentage drug remaining vs. time).
[b]Higushi kinetics (cumulative percentage drug released vs. square root of time).
[c]Korsmeyer kinetics (log cumulative percentage drug released vs. log time), with correlation values (r^2).

fitted a Fickian mode of diffusion (Ritger and Peppas, 1987). The zero order modeling showed low linearity (data not shown).

4. Discussion

Microparticles as drug carriers have the advantages of sustained or controlled release, the possibility of drug targeting to specific tissues, thus reducing side effects of drugs and improving their bioavailability. Therefore, microparticles as delivery systems have drawn much attention in the pharmaceutical field and have been successfully applied in several clinical trials. The goal of this study was to assess the possibility of the use of silk-derived fibroin as a microparticle carrier for the release of different BMPs.

Fibroin microspheres were manufactured in a semi-aqueous system, avoiding the use of toxic organic solvents, harsh conditions, cross-linking agents or surfactants, as a way of minimizing the risk of a loss of BMP activity during the particle preparation. The group of Kaplan and colleagues have recently reported that fibroin could form either particles or films with methanol and conserving the activity of incorporated drugs (Hofmann *et al.*, 2006; Wang *et al.*, 2007). When compared with other methods of processing, such as spray drying (Hino *et al.*, 2003), this approach not only avoids conditions unfavorable for the growth factor activity such as high temperature, but it also allows generating particles with smaller size.

The microparticles were easily prepared under sterile conditions and had a small size in a rather narrow size distribution. The size of particles was significantly smaller in the SEM counterpart images, probably due to the large swelling of the particles in the wet state. This was reported also in a former work (Cao *et al.*, 2007). The small particle size presented a double advantage, first by potentially enhancing the drug availability in the particle surface, and also by providing a surgical material that may be suitable for injectable implantation in bone defects in a slurry form. The BMPs were successfully encapsulated with a rather high efficiency, which is comparable to other works (Patel *et al.*, 2008; Wenk *et al.*, 2008). The lower encapsulation efficiencies observed for BMP-14 could be due to the differences in the BMP charge and its interaction with the fibroin material. Interestingly, this BMP has a lower isoelectric point when compared to BMP-2 (calculated using Expasy Proteomics tool Compute pI/Mw, at www.expasy.org; pI = 6.3 for BMP-2, pI = 5.9 for BMP-9 and pI = 5.8 for BMP-14). It is possible that this growth factor interacted to a weaker extent with the fibroin carrier since fibroin has an acidic isoelectric point (pI = 5.5).

During the initial stages of swelling, the fibroin microspheres showed substantial water uptake, mostly during the first two days of immersion, which also corresponded to the initial burst release, as the drug was rapidly released from the particles. Then, as swelling became gradually counterbalanced, the BMP was released slower and the release was mainly determined by the diffusion of the growth factor from the particle to the medium. It is possible that the erosion of the carrier contributed little to this, since we have found both that the release data best fitted with the Korsmeyer's equations and slope values between 0.30 and 0.42, thus indicating that the release was of a Fickian type of diffusion, controlled by only one mechanism and thus not dependent on carrier erosion (this applies when $n<0.43$, in the case of spherical particles) (Ritger and Peppas, 1987). In fact, as we have observed the silk fibroin microparticles exhibited a slow rate of degradation. The release amounts during this phase were such that they could meet the concentrations of growth factor required in most *in vitro* and *in vivo* applications (in the range of few hundreds of nanograms to a few micrograms), by choosing a specific amount of BMP during the loading process (Kenley *et al.*, 1994; Hosseinkhani *et al.*, 2007; Wei *et al.*, 2007; Bessa *et al.*, 2009).

The silk fibroin microspheres have shown to work as a microcarrier that provides a sustained release of the different BMPs in a timewise manner that could be used in bone regenerative applications. The bioactivity of the BMPs released from the silk fibroin microparticles will be explored in future works.

Acknowledgements

The authors wish to acknowledge Susana Moreira, Elsa Ribeiro and Katharina Schöbitz for critical input. This work was supported by Fundação para a Ciência e Tecnologia (PhD grant SFRH/BD/17049/2004), project ElastM

POCI/CTM/57177/2004 funded by FEDER and the Fundação para a Ciência e Tecnologia; Marie Curie Alea Jacta EST short-term grant (MEST-CT-2004-8104) and European STREP Project HIPPOCRATES (NMP3-CT-2003-505758). This work was carried out under the scope of the European NoE EXPERTISSUES (NMP3-CT-2004-500283).

Author Disclosure Statement

This study was performed according to ethical guidelines. No conflicts of interest exist.

References

Bessa PC, Cerqueira MT, Rada T, *et al*. 2009; Expression, purification and osteogenic bioactivity of recombinant human BMP-4, -9, -10, -11 and -14. *Protein Expr Purif* **63**: 89–94.

Bessa PC, Casal M, Reis RL. 2008a; Bone morphogenetic proteins in tissue engineering: the road from laboratory to the clinic, part I (basic concepts). *J Tissue Eng Regen Med* **2**: 1–13.

Bessa PC, Casal M, Reis RL. 2008b; Bone morphogenetic proteins in tissue engineering: the road from laboratory to the clinic, part II (BMP delivery). *J Tissue Eng Regen Med* **2**: 81–96.

Bourne DW. 2002; Pharmacokinetics. In *Modern Pharmaceutics*, Banker GS, Rhodes C (eds). Marcel Dekker: New York; 67–92.

Cao Z, Chen X, Yao J, *et al*. 2007; The preparation of regenerated silk fibroin microspheres. *Soft Matter* **3**: 910–915.

Chen FM, Wu ZF, Sun HH, *et al*. 2006; Release of bioactive BMP from dextran-derived microspheres: a novel delivery concept. *Int J Pharm* **307**: 23–32.

Chen FM, Zhao YM, Sun HH, *et al*. 2007; Novel glycidyl methacrylated dextran (Dex-GMA)/gelatin hydrogel scaffolds containing microspheres loaded with bone morphogenetic proteins: formulation and characteristics. *J Control Release* **118**: 65–77.

Chowdary KP, Ramesh KV. 1993; Studies on microencapsulation of diltiazem. *J Pharm Sci* **55**: 52–54.

Dines JS, Weber L. 2007; The effect of growth differentiation factor 5-coated sutures on tendon repair in a rat model. *J Shoulder Elbow Surg* **16**: S215–221.

Hadjiioannou TP, Christian GD, Koupparism MA. 1993; *Quantitative Calculations in Pharmaceutical Practice and Research*. VCH: New York; 345–348.

Higuchi T. 1963; Mechanism of sustained action medication. Theorical analysis of rate of release of solid drugs dispersed in solid matrices. *J Pharm Sci* **52**: 1145–1149.

Hino T, Tanimoto M, Shimabayashi S. 2003; Change in secondary structure of silk fibroin during preparation of its microspheres by spray-drying and exposure to humid atmosphere. *J Colloid Interface Sci* **266**: 68–73.

Hofmann S, Foo CT, Rossetti F, *et al*. 2006; Silk fibroin as an organic polymer for controlled drug delivery. *J Control Release* **111**: 219–27.

Hosseinkhani H, Hosseinkhani M, Khademhosseini A, *et al*. 2007; Bone regeneration through controlled release of bone morphogenetic protein-2 from 3D tissue engineered nano-scaffold. *J Control Release* **117**: 380–386.

Itoh S, Kikuchi M, Koyama Y, *et al*. 2004; Development of a hydroxyapatite/collagen nanocomposite as a medical device. *Cell Transpl* **13**: 451–461.

Kadomatsu H, Matsuyama T, Yoshimoto T, *et al*. 2008; Injectable growth/differentiation factor 5-recombinant human collagen composite induces endochondral ossification via Sry-related HMG box 9 (Sox9) expression and angiogenesis in murine calvariae. *J Periodont Res* **43**: 483–489.

Kang Q, Sun MH, Cheng H, *et al*. 2004; Characterization of the distinct orthotopic bone-forming activity of 14 BMPs using recombinant adenovirus-mediated gene delivery. *Gene Ther* **11**: 1312–1320.

Karageorgiou V, Meinel L, Hofmann S, *et al*. 2004; Bone morphogenetic protein-2 decorated silk fibroin films induce osteogenic differentiation of human bone marrow stromal cells. *J Biomed Mater Res A* **71**: 528–537.

Karageorgiou V, Tomkins M, Fajardo R, *et al*. 2006; Porous silk fibroin 3D scaffolds for delivery of bone morphogenetic protein-2 *in vitro* and *in vivo*. *J Biomed Mater Res A* **78**: 324–334.

Kenley R, Marden L, Turek T, *et al*. 1994; Osseous regeneration in the rat calvarium using novel delivery systems for recombinant human bone morphogenetic protein-2 (rhBMP-2). *J Biomed Mater Res* **28**: 1139–1147.

Kirker-Head C, Karageorgiou V, Hofmann S, *et al*. 2007; BMP–silk composite matrices heal critically sized femoral defects. *Bone* **41**: 247–255.

Lee SC, Shea M, Battle MA, *et al*. 1994; Healing of large segmental defects in rat femurs is aided by RhBMP-2 in PLGA matrix. *J Biomed Mater Res* **28**: 1149–1156.

Li C, Vepari C, Jin HJ, *et al*. 2006; Electrospun silk-BMP-2 scaffolds for bone tissue engineering. *Biomaterials* **27**: 3115–3124.

Merino R, Macias D, Gañan Y, *et al*. 1999; Expression and function of Gdf-5 during digit skeletogenesis in the embryonic chick leg bud. *Dev Biol* **206**: 33–45.

Nakamura T, Yamamoto M, Tamura M, *et al*. 2003; Effects of growth/differentiation factor-5 on human periodontal ligament cells. *J Periodontal Res* **38**: 597–605.

Nam J, Park YH. 2001; Morphology of regenerated silk fibroin: effects of freezing temperature, alcohol addition, and molecular weight. *J Appl Polym Sci* **81**: 3008–3021.

Nazarov R, Jin HJ, Kaplan DL. 2004; Porous 3D scaffolds from regenerated silk fibroin. *Biomacromolecules* **5**: 718–726.

Patel ZS, Yamamoto M, Ueda H, *et al*. 2008; Biodegradable gelatin microspheres as delivery systems for the controlled release of bone morphogenetic protein 2. *Acta Biomater* **4**: 1126–1138.

Phillips FM, Turner AS, Seim HB, *et al*. 2006; *In vivo* BMP-7 (OP-1) enhancement of osteoporotic vertebral bodies in an ovine model. *Spine J* **6**: 500–506.

Reddi AH. 2005; BMPs: from bone morphogenetic proteins to body morphogenetic proteins. *Cytokine Growth Factor Rev*, **16**: 249–250.

Ritger PL, Peppas NA. 1987; A simple equation for description of solute release. I. Fickian and non-Fickian release from non-swellable devices in the form of slabs, spheres, cylinders or discs. *J Control Release* **5**: 23–26.

Scheibel T. 2006; Silk: a biomaterial with several facets. *Appl. Phys A* **82**: 191–196.

Simank HG, Herold F, Schneider M, *et al*. 2004; Growth and differentiation factor 5 (GDF-5) composite improves the healing of necrosis of the femoral head in a sheep model. Analysis of an animal model. *Orthopade* **33**: 68–75.

Spiro RC, Thompson AY, Poser JW. 2001; Spinal fusion with recombinant human growth and differentiation factor-5 combined with a mineralized collagen matrix. *Anat Rec* **263**: 388–395.

Tamada Y. 2005; New process to form a silk fibroin porous 3D structure. *Biomacromolecules* **6**: 3100–3106.

Wang X, Wenk E, Matsumoto A, *et al*. 2007; Silk microspheres for encapsulation and controlled release. *J Control Release* **117**: 360–370.

Wang YJ, Lin FH, Sun JS, *et al*. 2003; Collagen–hydroxyapatite microspheres as carriers for bone morphogenic protein-4. *Artif Organs* **27**: 162–168.

Wei G, Jin Q, Giannobile WV, *et al*. 2007; The enhancement of osteogenesis by nanofibrous scaffolds incorporating rhBMP-7 nanospheres. *Biomaterials* **28**: 2087–2096.

Wenk E, Wandrey AJ, Merkle HP, *et al*. 2008; Silk fibroin spheres as a platform for controlled drug delivery. *J Control Release* **132**: 26–34.

Zhang YQ, Shen WD, Xiang RL, *et al*. 2007; Formation of silk fibroin nanoparticles in water-miscible organic solvent and their characterization. *J Nanopart Res* **9**: 885–900.